Amplification of information transfer in excitable systems that reside in a steady state near a bifurcation point to complex oscillatory behavior

Matjaž Perc* and Marko Marhl
Department of Physics, Faculty of Education, University of Maribor, Koroška cesta 160, SI-2000 Maribor, Slovenia
(Received 27 July 2004; published 16 February 2005)

We study the amplification of information transfer in excitable systems. We show that excitable systems residing in a steady state near a bifurcation point to complex oscillatory behavior incorporate several frequencies that can be exploited for a resonant amplification of information transfer. In particular, for excitable neurons that reside in a steady state near a bifurcation point to elliptic bursting oscillations, we show that in addition to the resonant frequency of damped oscillations around the stable focus, another frequency exists that resonantly enhances large amplitude bursts and thus amplifies the information transfer in the system. This additional frequency cannot be found by the local stability analysis and has never been used for amplifying the information transfer in a system. The results obtained for elliptic bursting oscillations can be generalized also to other complex oscillators, such as parabolic or square-wave bursters. Additionally, the biological importance of presented results in the field of neuroscience is outlined.

DOI: 10.1103/PhysRevE.71.026229 PACS number(s): 05.45.−a, 05.40.Ca

I. INTRODUCTION

Responses of excitable systems to external perturbations are of key importance for understanding mechanisms of signal transduction in a broad variety of natural as well as artificial systems. Particularly in biological systems, it is of special importance to understand the response of a given system to an external signal since thereon often relies proper functioning of the whole organism. For example, external signals that assure signal transduction and information processing are very important for normal functioning of a single cell as well as coupled cells in the tissue [1].

In order to guarantee low energy consumption and hence optimal functioning, external signals acting upon an excitable system are usually weak. This seems contradictory, since in order to assure reliable signal transduction and information processing, external signals also have to act very convincingly. While studying this apparent contradiction, scientists have encountered a fascinating phenomenon termed stochastic resonance [2]. The main virtue of stochastic resonance is the exploitation of noisy perturbations for constructive purposes, in particular by enhancing weak external signals, thereby assuring enhanced information transfer in the system. This constructive role of noise was initially encountered in bistable systems [3], and later confirmed theoretically as well as experimentally in a broad variety of physical [2,4,5] and biological systems [6–12].

Recently, stochastic resonance effects have been studied intensely in excitable systems that reside in a steady state very close to the oscillatory regime [13–21]. These excitable steady states are especially relevant in nature, where it is often the case that quiescence has to be abruptly replaced by oscillatory behavior upon detection of a weak external stimuli. Mathematically, this is feasible when the system with oscillatory states is waiting in an excitable steady state that is very close to the bifurcation point.

Functioning of neurons, for example, is often described as a continuous switching between a quiescent and an oscillatory state that are separated by a bifurcation point [22]. For special types of bifurcation points the system can be easily, i.e., already with a weak external signal, forced from the quiescent to the oscillatory state, which is the intuitive definition of excitability [22,23]. Excitable neurons in a quiescent state often express damped or sustained small-amplitude oscillations of membrane potential. This dynamical property makes neurons especially sensitive to external signals with a particular frequency and/or amplitude, and hence promotes diversity in response of the system with respect to the applied forcing [24]. These diversities arise due to the occurrence of classical resonance between the system and the external signal. The fact that excitable systems are more sensitive to some external signals than others has motivated several studies, in particular analyzing the possibilities of amplifying the stochastic resonance effects, thus assuring an enhanced noise-induced information transfer in the system [25–28].

The basic idea behind the amplification of stochastic resonance is to combine the stochastic resonance with classical resonance effects. For bistable systems, Gammaitoni *et al.* [25] introduced an open-loop control scheme that permits the enhancement or suppression of the spectral response to threshold-crossing events by injection of an additional periodic signal. The amplification of stochastic resonance effects in bistable systems was coined as the “control of stochastic resonance” [25]. Excitable systems near a bifurcation point to the oscillatory regime were also studied under the influence of periodic perturbations. The amplitude and/or frequency of the external periodic perturbation were taken as variable parameters while looking for an optimal interplay between classical resonance effects and noise-induced re-

*Corresponding author. Present address: University of Maribor, Department of Physics, Faculty of Education, Koroška cesta 160, SI-2000 Maribor, Slovenia Electronic address: matjaz.perc@uni-mb.si

sponses of the system that would in turn lead to the maximal amplification of information transfer. It has been shown, for example, that an optimal amplitude of a high-frequency periodic forcing can resonantly enhance the response of an excitable system to a low-frequency signal [28]. Thereby, the resonance-like behavior of the system with respect to the amplitude of the high frequency forcing, i.e., vibrational resonance was exploited. A conceptually similar phenomenon was observed with respect to the variable frequency of a high-frequency periodic forcing. Parmananda *et al.* [26] have shown that an optimal frequency of a high-frequency periodic forcing can also resonantly amplify information transfer in the system. The optimal frequency of the external forcing corresponds to the frequency of damped oscillations around the steady state, i.e., the stable focus, of the excitable autonomous system. This is directly linked to the fact that the excitable system is in resonance with the external signal that has the same frequency as the damped small-amplitude oscillations around the stable focus. The latter frequency can be easily estimated from the imaginary part of eigenvalues of the flow dynamics linearized around the steady state [24,26,29,30].

An extension of this basic concept was recently proposed in [27], where it was shown that the effect of stochastic resonance can also be amplified by the addition of a high-frequency signal if the latter is in resonance with the so-called Canard oscillations of the system. The Canard effect relates to a specific behavior of the system at the bifurcation point to the oscillatory regime. The main feature of this phenomenon is that a very small change in the bifurcation parameter leads to a large difference in the behavior of the system [31–33]. Thus, amplitudes and frequencies of oscillations in this small parameter range change abruptly. The high frequency of these oscillations is in the context of Volkov *et al.* [27] used for aim-oriented amplification of noise-induced information transfer in the system, i.e., the so-called Canard-enhanced stochastic resonance.

In this paper, we further complement the existing mechanisms that can be exploited for amplifying the information transfer in excitable systems. In addition to the local stability analysis of the autonomous system, which gives an insight into the possible resonant frequencies characteristic for the phase space in the vicinity of the steady state, we are interested in the global characteristics of the phase space. This is of particular importance for excitable steady states close to bifurcation points that lead to complex oscillatory behavior, which is often characterized with several different intrinsic frequencies. Since the excitable steady state is very close to the bifurcation point, and hence to the oscillatory states, the phase space around the excitable state must have very similar characteristics as the phase space beyond the bifurcation point, assuming, of course, that the transition through the bifurcation is smooth, i.e., no catastrophes occur [22]. Although the local stability analysis of the excitable state reveals only one characteristic frequency, which is the one of the stable focus, the system may indeed posses several other "global-resonant" frequencies that can also be used for the amplification of the information transfer. We demonstrate how these additional resonant frequencies can be determined by calculating the Fourier coefficients [34] of noise-induced oscillations under the influence of subthreshold periodic forcing.

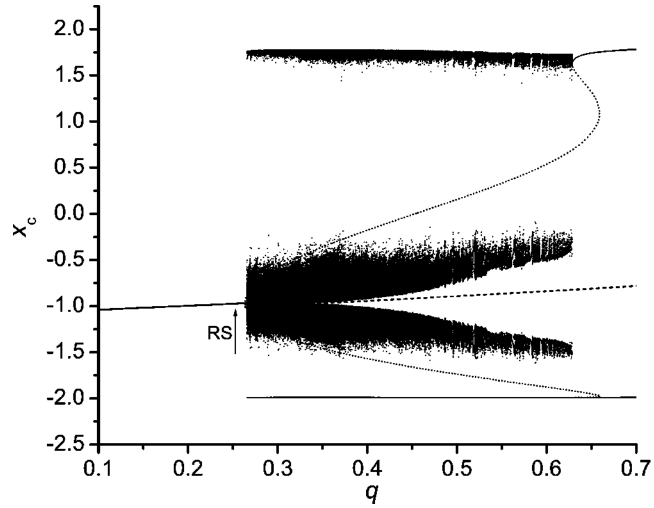

FIG. 1. Bifurcation diagram of the autonomous mathematical model. In dependence on parameter q, the characteristic values (x_c) of variable $x(t)$ are presented: stable (solid line) and unstable (dashed line) foci, maxima, and minima of unstable (dotted lines) and stable (dots) periodic solutions. The arrow marks the reference state (RS). For further details and parameter values see text.

For a mathematical model of an excitable neuron [35], we prove the existence of additional resonant frequencies for a steady state near a bifurcation point to elliptic bursting behavior, which is one of several possible bursting types [22,36,37]. More precisely, there are two resonant frequencies in our system; one matching the frequency of damped oscillations around the steady state (stable focus), and the second that resonantly enhances large amplitude bursts. While the external signal with the first frequency resonantly helps to lower the threshold for neuron firing, the second frequency plays a crucial role in maintaining a well-expressed bursting phase of oscillations. The latter effect is of key importance for bursting oscillations, since well-expressed bursts of action potential are vital for increased reliability of synaptic transmission [38], and may also provide effective mechanisms for selective communication between neurons [39,40]. The results obtained here for elliptic bursting oscillations may be of even greater importance also for other bursting types, such as parabolic or square-wave bursting, were the oscillatory convergence to the rest state is, due to a different bifurcation structure [22], not inherently present in the system, and thus only the "global-resonant" frequencies determined as described below, may be exploited for the amplification of information transfer in the system.

The paper is structured as follows. Section II is devoted to the description of the mathematical model and its main characteristics. In Sec. III we point out similarities between the noise-induced oscillations from the steady state and the autonomous oscillatory behavior, whereas in Sec. IV the main results are presented. In Sec. V we summarize the results and outline the biological importance of our findings.

II. MODEL

We study a mathematical model of an idealized nerve membrane model, which was formulated by FitzHugh and

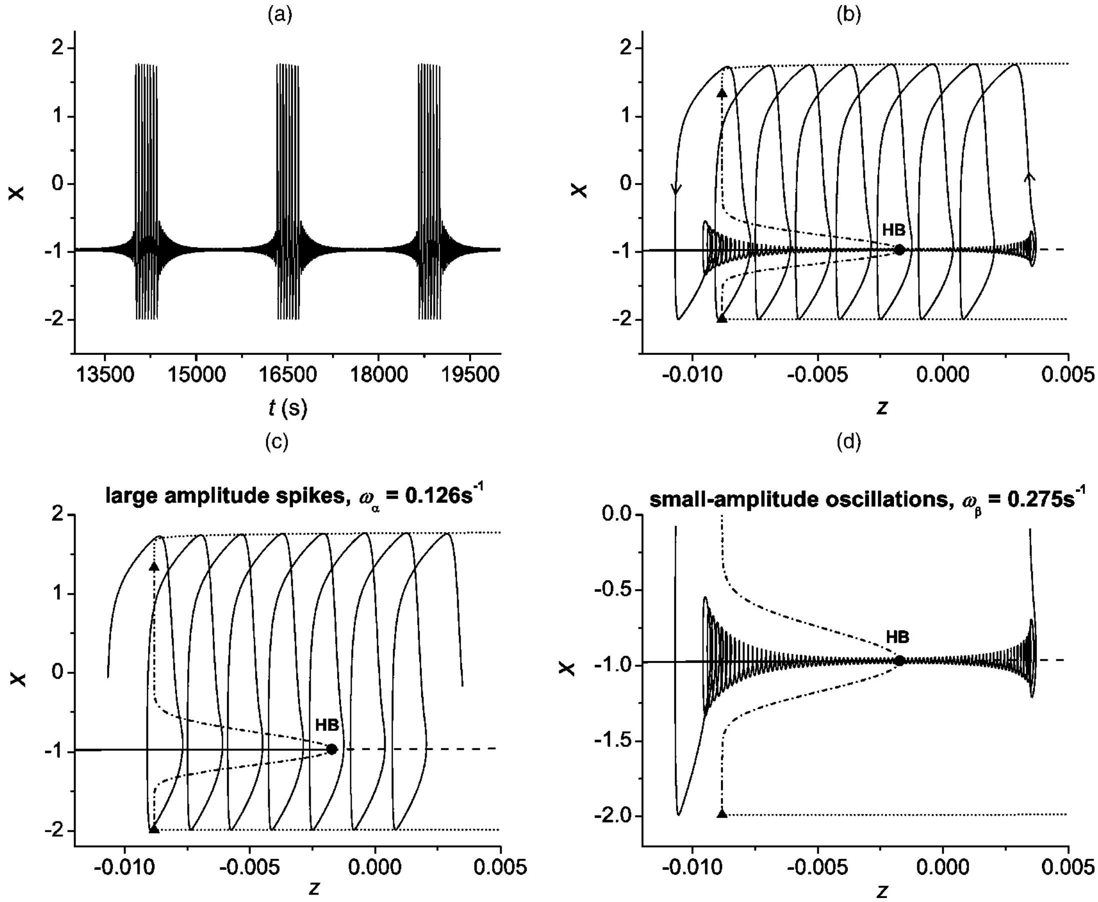

FIG. 2. Analysis of autonomous bursting oscillations at $q=0.33$: (a) time course of variable x; (b) 2D projection of the attractor and the corresponding bifurcation diagram. Solid (dashed) lines represent stable (unstable) foci, whereas dotted (dashed–dotted) lines represent stable (unstable) periodic solutions. Up-triangles denote the fold limit cycle bifurcation and the circle denotes the subcritical Hopf bifurcation (HB); (c) separately shown large amplitude spikes during the bursting phase; and (d) small-amplitude oscillations during the slow passage phase.

Rinzel in 1976 and later extensively studied in [35]. The evolution of the FitzHugh-Rinzel (FHR) model is governed by the differential equations

$$\frac{\mathrm{d}x}{\mathrm{d}t} = x - x^3/3 - y + z + q, \tag{1}$$

$$\frac{\mathrm{d}y}{\mathrm{d}t} = \delta(x + a - by), \tag{2}$$

$$\frac{\mathrm{d}z}{\mathrm{d}t} = \varepsilon(-x + c - dz). \tag{3}$$

For parameter values $a=0.7$, $b=0.8$, $c=-0.9$, $d=1$, $\delta=0.08$, and $\varepsilon=0.0001$, the system has a Hopf bifurcation at $q=0.2637$. For $q<0.2637$ the system is quiescent whereas for $q>0.2637$ the system exhibits elliptic bursting oscillations that transient to simple spikelike oscillations as q is further enlarged. The bifurcation diagram of the system is presented in Fig. 1, where the characteristic values (x_c) of variable $x(t)$ [see Eq. (1)] are depicted in dependence on the parameter q. Stable and unstable foci are presented by solid and dashed lines, respectively, whereas dotted lines indicate maxima, and minima of unstable limit cycles. For stable periodic solutions, maxima and minima of $x(t)$ are depicted by dots. To point out the complexity of bursting oscillations for $q>0.2637$, in addition to the main maxima and minima belonging to large amplitude spikes, also maxima and minima of small amplitude oscillations that appear in the bursting pattern are presented. The arrow at $q=0.25$ marks the excitable steady state, which is taken as the reference state (RS) for our analyses in the subsequent sections.

To reveal the main characteristics of elliptic bursting oscillations, we consider autonomous oscillations of the system at $q=0.33$, which are presented in Fig. 2(a). The 2D projection of the corresponding attractor in the phase space, together with the bifurcation diagram obtained according to the fast-slow subsystem method proposed by Rinzel [35], is presented in Fig. 2(b). The virtue of the fast-slow subsystem method is to extract the fast changing variables of the system and then use the slow changing variables as bifurcation parameters. The fast changing variables of the FHR model were identified to be $x(t)$ and $y(t)$, whereas the slow changing variable is $z(t)$. Hence, we can reduce the 3D system $(x(t),y(t),z(t))$ to a 2D system $(x(t),y(t))$ and use the variable $z(t)$ as the bifurcation parameter. The bifurcation analy-

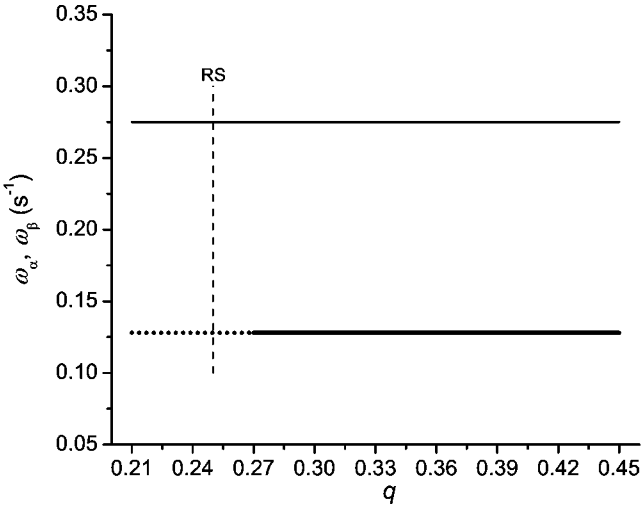

FIG. 3. Frequency of large amplitude spikes ω_α (thick solid line) and small-amplitude oscillations ω_β (thin solid line) in dependence on the parameter q. The dotted line indicates hypothesized values of ω_α, whereas the vertical dashed line marks the reference state (RS).

sis was carried out with the software package AUTO97 [41]. It can be well observed that the transition to repetitive spiking occurs via a subcritical Hopf bifurcation (HB) and the transition to the quiescent state occurs via a fold limit cycle bifurcation, which is the characteristic bifurcation structure of elliptic bursting oscillations [22,35]. Noteworthy, the oscillatory state is characterized by the slow passage effect [37,42,43], which manifests as a delayed transition of the trajectory to the upper stable periodic branch after the subcritical Hopf bifurcation is exceeded. The most interesting feature of the system, however, that is of particular relevance for this study is the inherent presence of two high frequencies in the system; namely the frequency of large amplitude spikes during the bursting phase [Fig. 2(c)] and the frequency of small-amplitude oscillations during the slow passage phase [Fig. 2(d)]. The angular frequency of large amplitude spikes matches the frequency of stable periodic branches $\omega_\alpha = 0.126\ \text{s}^{-1}$, whereas the angular frequency of small-amplitude oscillations matches the frequency of stable/unstable foci in the 2D bifurcation diagram, which can be obtained from the complex conjugate eigenvalues at the HB ($\lambda_{1,2} = \pm 0.275\, i \Rightarrow \omega_\beta = 0.275\ \text{s}^{-1}$).

While for different values of the parameter $q > 0.2637$ oscillations differ considerably in their main frequency at which successive bursting phases occur, frequencies ω_α and ω_β remain constant, as shown in Fig. 3. Moreover, the frequency ω_β of small-amplitude oscillations in the oscillatory regime at $q > 0.2637$ is also characteristic for damped oscillations around the stable foci for $q < 0.2637$. This indicates that the phase space topology varies only little while q passes through the Hopf bifurcation, which means that the phase space at $q < 0.2637$ has very similar topological properties as the phase space at $q > 0.2637$. Therefore, we hypothesize that also the frequency of large amplitude spikes, ω_α, is inherently incorporated in the phase space already at $q < 0.2637$ (dotted line in Fig. 3), as the so-called "global-resonant" frequency of unstable periodic orbits (UPOs), which can be observed if the system is externally perturbed from the excitable reference state. The existence of these UPOs, however, cannot be determined by the local stability analysis. Nevertheless, their presence can be justified by considering the fact that the bifurcation responsible for the onset of bursting oscillation is noncatastrophic, and thus the phase space varies smoothly not just locally around the steady state, but also globally. Therefore, if the phase space topology is indeed very similar for all values of q around the bifurcation point, it is reasonable to expect that an external forcing with the "global-resonant" frequency of UPOs would elicit a resonant response of the system. In the following, we confirm this reasoning by studying solely noise-induced oscillations from the RS, and show that both frequencies (ω_α and ω_β) can indeed be exploited for the amplification of information transfer in the system.

III. NOISE-INDUCED OSCILLATIONS

The Gaussian noise, $\zeta(t)$, with the variance σ is applied to the excitable RS by adding $\zeta(t)$ as an additional term to Eq. (1). For $\zeta(t) = 0$ the system remains quiescent, whereas if the noise variance is set large enough, the system exhibits noise-induced bursting oscillations. Thus, the initially quiescent system at $q = 0.25$ can be excited solely by noise if σ is chosen large enough. The time course of purely noise-induced oscillations and the corresponding fast-Fourier transform (FFT) are shown in Figs. 4(a) and 4(b), respectively. It can be well observed that the noise-induced oscillations are characterized by three well-expressed angular frequencies (ω_0, ω_1, and ω_2), namely the predominant frequency of the main bursting pattern ($\omega_0 \approx 4.9 \times 10^{-3}\ \text{s}^{-1}$), the frequency of large amplitude spikes during the bursting phase ($\omega_1 \approx 0.13\ \text{s}^{-1}$), and the frequency of small amplitude oscillations that emerge between successive bursting phases and corresponds to the frequency of damped oscillations around the stable focus at $q = 0.25$ ($\omega_2 \approx 0.26\ \text{s}^{-1}$). While the low interburst frequency ω_0 depends significantly on the noise intensity, i.e., increases/decreases with increasing/decreasing σ, both high frequencies remain virtually unaffected by varying σ. As hypothesized above, both high frequencies in the noise-driven system are very similar to those found in the deterministic oscillatory states ($\omega_1 \approx \omega_\alpha$ and $\omega_2 \approx \omega_\beta$), which confirms the above prediction that the phase space at the RS has very similar topological properties as the phase space beyond the Hopf bifurcation ($q > 0.2637$). Thus, the phase space around the excitable reference state (see Fig. 1) indeed incorporates UPOs with two high frequencies (ω_1 and ω_2) that may potentially be exploited for the oscillatory amplification of information transfer in the system.

IV. AMPLIFICATION OF INFORMATION TRANSFER

The oscillatory amplification of noise-induced information transfer can occur when the system is, in addition to noise and the low-frequency information-carrying signal, driven with a high-frequency periodic signal with frequency Θ that matches some intrinsic frequency (ω) that is incorporated in the system. Only those frequencies Θ that are close

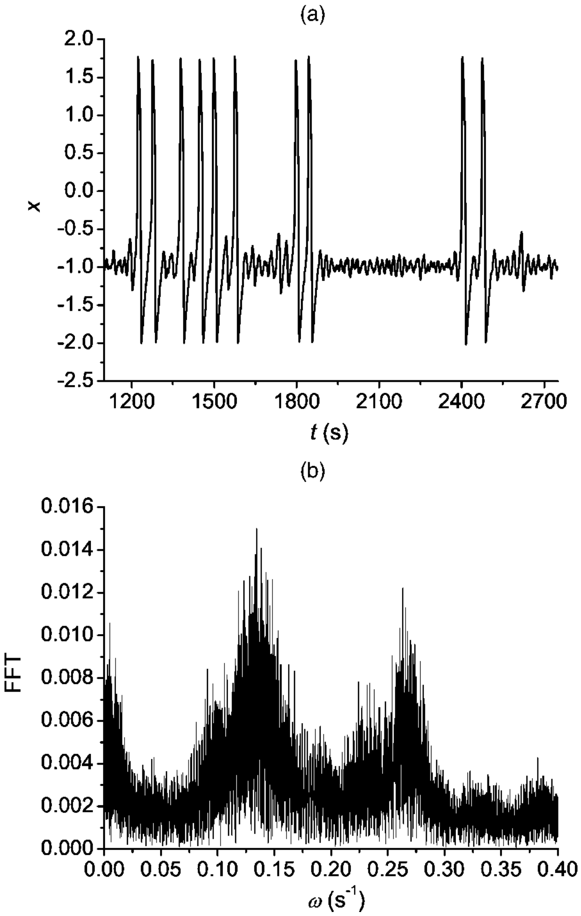

FIG. 4. Analysis of noise-induced oscillations from the RS for $\sigma=0.05$: (a) time course of variable x; (b) the corresponding fast-Fourier transform.

to some intrinsic frequency of the system, i.e., $\Theta \approx \omega$, can successfully evoke a resonant response and in turn lead to the amplification of information transfer. To study the oscillatory amplification of information transfer, we add an additional term $S(t)$ to Eq. (1), while Eqs. (2) and (3) remain unchanged. The additional term $S(t)$ added to Eq. (1) is defined as

$$S(t) = \zeta(t) + \kappa \sin(\Omega t) + \Lambda \sin(\Theta t), \tag{4}$$

where $\zeta(t)$ is the Gaussian noise with variance σ, $\kappa \sin(\Omega t)$ is the information carrying low-frequency signal, and $\Lambda \sin(\Theta t)$ is the high-frequency signal responsible for the oscillatory amplification of the information transfer. In all subsequent calculations, κ and Λ are set small enough so that if $\sigma=0$, the system remains quiescent. Figure 4 shows that the RS of the noise-driven FHR model incorporates two high frequencies (ω_1 and ω_2) that may potentially be exploited for the oscillatory amplification of information transfer by setting $\Theta=\Theta_1 \approx \omega_1$ or $\Theta=\Theta_2 \approx \omega_2$ in Eq. (4).

In order to determine these two frequencies (Θ_1 and Θ_2) more precisely, we systematically investigate responses of the system to a high-frequency sinusoidal forcing in the presence of noise. To this purpose we set $\kappa=0$, and $\Lambda=0.01$ in Eq. (4), whereas the frequency of the sinusoidal forcing Θ

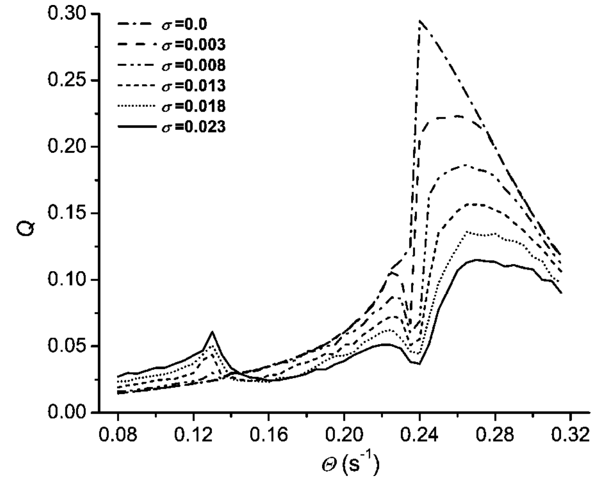

FIG. 5. Fourier coefficients for the periodically driven ($\kappa=0, \Lambda=0.01$) FHR model from the RS under the influence of different noise intensities.

and the noise variance σ are varied. Note, that in this case the amplitude of the sinusoidal forcing Λ is also set small enough so that the system does not express large amplitude bursting oscillations without the addition of noise. To evaluate responses of the periodically driven noisy system in dependence on Θ, we calculate the Fourier coefficients Q. The Fourier coefficients tell precisely how much information in the signal is transported with a particular forcing frequency [2]. Noteworthy, the Fourier coefficients are proportional to the (square of the) spectral power amplification (SPA) [45], which is often used as a measure for stochastic resonance. Here, the Fourier coefficients Q are calculated according to the equations [34]:

$$Q_{\sin} = \frac{\Theta}{2n\pi}\int_0^{2\pi n/\Theta} 2x(t)\sin(\Theta t)\mathrm{d}t, \tag{5}$$

$$Q_{\cos} = \frac{\Theta}{2n\pi}\int_0^{2\pi n/\Theta} 2x(t)\cos(\Theta t)\mathrm{d}t, \tag{6}$$

$$Q = \sqrt{Q_{\sin} + Q_{\cos}}. \tag{7}$$

We calculate the Fourier coefficients Q in dependence on the frequency Θ for various noise intensities σ. Results presented in Fig. 5 are in excellent agreement with the results presented in Figs. 3 and 4, and enable us to precisely determine both frequencies that are inherently present in the system at the RS. The first peak at $\Theta_1=0.131\ \mathrm{s}^{-1}$ corresponds to the frequency of large amplitude spikes during the bursting phase, whereas the second peak at $\Theta_2=0.256\ \mathrm{s}^{-1}$ corresponds to the frequency of small-amplitude oscillations that emerge between successive bursting phases, also called the frequency of the oscillatory convergence to the rest state.

It remains to verify if both frequencies (Θ_1 and Θ_2) assure the amplification of information transfer with respect to the low-frequency information carrying signal $\kappa \sin(\Omega t)$, which has been excluded from the calculations ($\kappa=0$) until now. To this purpose we calculate the Fourier coefficients Q with

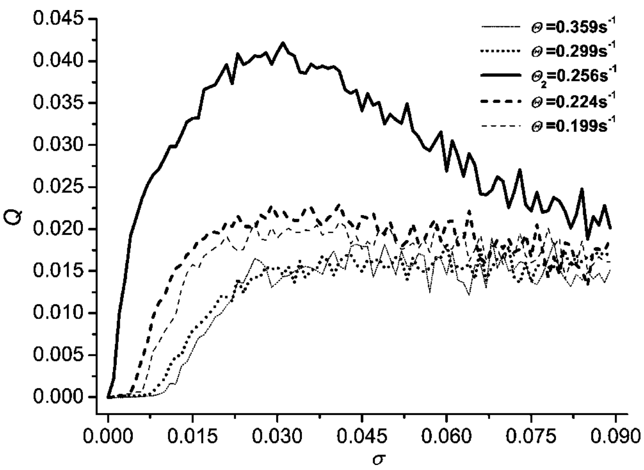

FIG. 6. Fourier coefficients calculated with respect to the information-carrying frequency $\Omega = 3.14 \times 10^{-3}$ s^{-1} ($\kappa = 0.005$) under the influence of a high-frequency periodic forcing ($\Theta \cong \Theta_2, \Lambda = 0.01$) in dependence on the noise intensity.

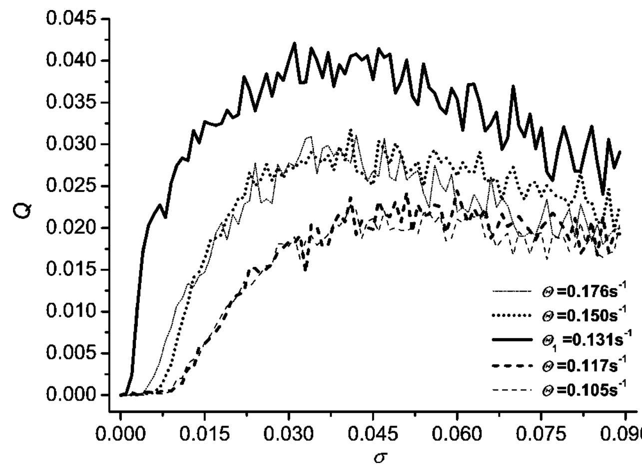

FIG. 7. Fourier coefficients calculated with respect to the information-carrying frequency $\Omega = 3.14 \times 10^{-3}$ s^{-1} ($\kappa = 0.005$) under the influence of a high-frequency periodic forcing ($\Theta \cong \Theta_1, \Lambda = 0.02$) in dependence on the noise intensity.

respect to the information carrying frequency Ω, but consider only large amplitude spikes as possible information carriers, whereas the small-amplitude oscillations between successive bursting phases are replaced by the steady state value of the autonomous system at the RS. The threshold for large amplitude spikes is set to $x = 0.0$. Thereby, we achieve that if no noise is added to the system the Fourier coefficients are zero, since no information transport occurs. Noteworthy, an identical approach has already been used by Volkov *et al.* [27].

First, we calculate the Fourier coefficients Q for frequencies around $\Theta_2 = 0.256$ s^{-1} to verify if an enhanced information transport, i.e., amplified stochastic resonance, can be obtained near this resonant frequency. To this purpose we set $\Omega = 3.14 \times 10^{-3}$ s^{-1}, $\kappa = 0.005$ and $\Lambda = 0.01$ in Eq. (4), whereas Θ is varied around Θ_2. The results are presented in Fig. 6. It can be well observed that Θ_2 indeed warranties an enhanced information transport in the system at frequency $\Omega = 3.14 \times 10^{-3}$ s^{-1} already at low noise intensities. On the other hand, any other frequency around Θ_2 does not have the same effect even at higher noise intensities. Thus, we conclude that the addition of a periodic forcing with the resonant frequency Θ_2 indeed amplifies the stochastic resonance, and thus guarantees an enhanced information transfer in the examined system.

Next, let us examine if the resonant frequency $\Theta_1 = 0.131$ s^{-1}, termed above as the "global-resonant" frequency, also assures an amplified information transfer in the system. To this purpose we calculate the Fourier coefficients Q according to Eqs. (5)–(7) by taking $\Omega = 3.14 \times 10^{-3}$ s^{-1}, $\kappa = 0.005$, and $\Lambda = 0.02$, in Eq. (4). Note, that the amplitude of the high-frequency sinusoidal signal Λ can be set larger than in the previous case ($\Lambda = 0.01$), since Θ_1 is not in resonance with the frequency of the oscillatory convergence to the rest state, and thus doesn't amplify the rest state as much as the sinusoidal forcing with frequency Θ_2. The obtained results for various Θ around Θ_1 are presented in Fig. 7. It is evident that the resonant frequency $\Theta_1 = 0.131$ s^{-1}, corresponding to the frequency of large amplitude spikes during the bursting phase, similarly as the frequency of the convergence to the rest state Θ_2, also assures an enhanced information transport in the system at frequency $\Omega = 3.14 \times 10^{-3}$ s^{-1} already at low noise intensities. Finally, we may conclude that both frequencies that are inherently present in the system at the RS assure the amplification of stochastic resonance effects, and thus guarantee an enhanced information transport in the system.

Despite the relative well-expressed resemblance of the results presented in Figs. 6 and 7, the mechanism behind the amplification of information transfer in the system is quite different for both resonance frequencies. The reason for this difference lies in the origin of the resonant frequencies Θ_1 and Θ_2 in the system. While Θ_1 represents the frequency of large amplitude spikes during the bursting phase, Θ_2 represents the frequency of small amplitude oscillations between successive bursting phases. Therefore, the inclusion of an additional sinusoidal forcing with the frequency Θ_2 resonantly (far more than any other frequency around Θ_2) amplifies the steady state and thus lowers the threshold, whereas the inclusion of an additional sinusoidal forcing with the frequency Θ_1 does not have the same effect. It is still true, of course, that Θ_1 excites the steady state of the system and thus lowers the threshold, but not in a resonant manner, i.e., not more than any other frequency around Θ_1 used for the calculations presented in Fig. 7. Hence, the oscillatory amplification of information transfer presented in Fig. 7 requires a different reasoning than the one presented in Fig. 6.

We emphasize, that the oscillatory amplification of information transfer with Θ_1 sets into action after the first noise-induced bursting phases in the system emerge. Only then, the sinusoidal signal with Θ_1 is able to resonantly (far more than any other frequency around Θ_1) enhance the initially noise-induced bursting phase and thereby assure an enhanced information transport in the system. This explanation can be well corroborated by studying time courses of noise-induced oscillations under the influence of a subthreshold bichromatic signal [Eq. (4)], as presented in Fig. 8. It can be well observed that the steady state in Fig. 8(a) ($\Theta = \Theta_2, \Lambda = 0.01$) is more excited than the one in Fig. 8(b) ($\Theta = \Theta_1, \Lambda = 0.02$), despite the fact that the amplitude of the high-frequency sig-

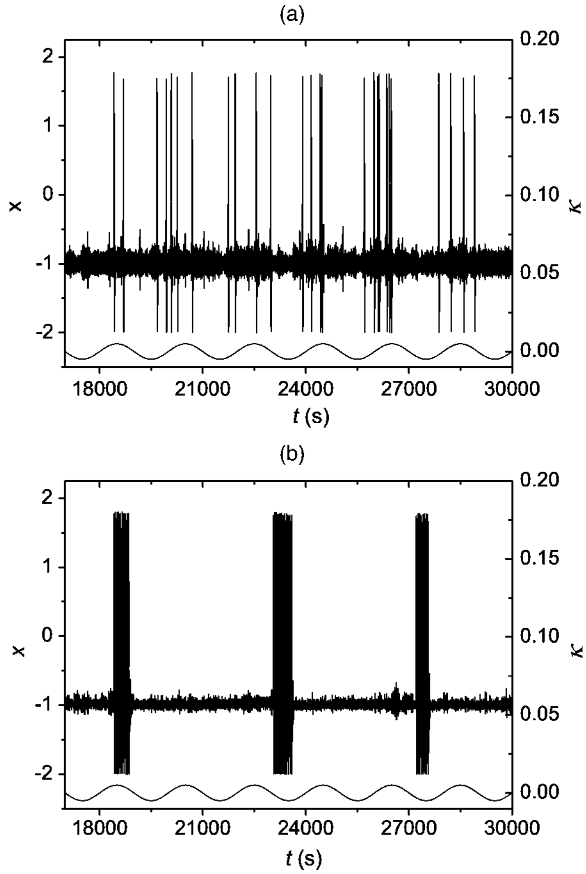

FIG. 8. Bursting oscillations induced from the RS for $\sigma=0.03$, under the influence of a subthreshold bichromatic signal: (a) time course of variable x for $\Theta=\Theta_2$ and $\Lambda=0.01$; (b) time course of variable x for $\Theta=\Theta_1$ and $\Lambda=0.02$. In both cases $\Omega=3.14\times10^{-3}\ \mathrm{s}^{-1}$ and $\kappa=0.005$.

nal was two times larger in the later case. Consequently, bursting phases in Fig. 8(a) occur more frequently, i.e., almost at all maxima of $\kappa\sin(\Omega t)$, than in Fig. 8(b), but are, however, far less pronounced than in the case of resonant enhancement with $\Theta=\Theta_1$.

Furthermore, it is important to point out that oscillations in Fig. 8(b) resemble the deterministic ones presented in Fig. 2(a) much better than the oscillations in Fig. 8(a). Thus, it may be concluded that the oscillations with resonantly enhanced bursting phases ($\Theta=\Theta_1$) are more likely to fulfill their established biological role, which is increase the reliability of synaptic transmission [38] as well as provide effective mechanisms for selective communication between neurons [39,40].

V. SUMMARY

In the paper, a new mechanism for amplifying the information transfer in excitable systems close to bifurcation points that lead to complex oscillatory behavior is presented. We show that, under the assumption of a smooth, i.e., noncatastrophic, transition through the bifurcation point from the quiescent to the oscillatory regime, the phase space at the excitable steady state has very similar characteristic as at the oscillatory states beyond the bifurcation. Therefore, such excitable systems incorporate several intrinsic frequencies that can be exploited for the amplification of information transfer. In particular, for an excitable steady state close to elliptic bursting behavior, we show that the phase space is characterized by two high frequencies that are both suitable for the amplification of information transfer. While the frequency of damped small-amplitude oscillations around the stable focus can be determined by the local stability analysis, and was already used before for the amplification of stochastic resonance [26], the second frequency is characteristic for the global phase space, and thus cannot be determined by the local stability analysis. Instead, the second frequency, conveniently termed as the “global-resonant” frequency due to its inherent presence in the global phase space as opposed to the frequency of damped oscillations existing in the local vicinity of the steady state, can be precisely extracted from the quiescent system by calculating the Fourier coefficients of noise-driven oscillations under the influence of a variable high-frequency forcing. We show that this “global-resonant” frequency can be exploited for the amplification of information transfer in the system just as successfully as the frequency of damped oscillations around the steady state.

It should be emphasized, that such “global-resonant” frequencies might be particular important also for other complex oscillators, such as parabolic or square-wave bursters. There, the quiescent state of the system is not a stable focus, but a stable node. Consequently, such systems do not possess damped small-amplitude oscillations around the steady state, whose frequency could be revealed by the local stability analysis. Hence, the “global-resonant” frequencies are in this case the only remaining candidates available to elicit a resonant response of the system, and in turn amplify the information transfer.

Another important aspect of the presented results is the fact that the amplification of information transfer with the “global-resonant” frequency of large amplitude spikes seems to produce biologically more relevant oscillations than the previously known mechanism [26]. In particular, the resonant enhancement of the bursting phase manifests in an increased number of spikes during a particular bursting phase, as well as a better-pronounced predominant frequency between consecutive spikes. Indeed, it was recently argued that the postsynaptic response of neurons could depend significantly on the frequency content of the burst, due to the existence of a frequency preference at the synaptic as well as cellular level. Since different neurons possess different resonant frequencies, the same burst can be resonant for one cell and not resonant for another, thereby eliciting responses selectively in one cell but not the other. Hence, the number of spikes in a burst as well as its frequency content might be crucial, either for assuring selective communication between neurons [39,40], or for the constructive contribution to synchronization and neuronal processing [1,44,46]. Our theoretical findings fully confirm the above described reasoning and hopefully outline some possibilities for further experimental work, especially in the field of neuroscience, where bursting oscillations were found to be of special importance.

[1] F. C. Hoppensteadt and E. M. Izhikevich, *Weakly Connected Neural Networks* (Springer, Berlin, 1997).
[2] L. Gammaitoni, P. Hänggi, P. Jung, and F. Marchesoni, Rev. Mod. Phys. **70**, 223 (1998).
[3] R. Benzi, A. Sutera, and A. Vulpiani, J. Phys. A **14**, L453 (1981).
[4] L. Gammaitoni, Phys. Rev. E **52**, 4691 (1995).
[5] V. V. Osipov and E. V. Ponizovskaya, JETP Lett. **70**, 425 (1999).
[6] J. K. Douglass, L. A. Wilkens, E. Pantazelou, and F. Moss, Nature (London) **365**, 337 (1993).
[7] H. A. Braun, H. Wissing, K. Schäfer, and M. C. Hirsch, Nature (London) **367**, 270 (1994).
[8] D. Russel, L. Wilkens, and F. Moss, Nature (London) **402**, 291 (1999).
[9] E. Manjarrez, J. G. Rojas-Piloni, I. Méndez, L. Martínez, D. Vélez, D. Vázquez, and A. Flores, Neurosci. Lett. **326**, 93 (2002).
[10] E. Manjarrez, O. D. Martnez, I. Mendez, and A. Flores, Neurosci. Lett. **324**, 213 (2002).
[11] P. Hänggi, Chem. Phys. **3**, 285 (2002).
[12] S. Reinker, E. Puil, and R. M. Miura, Bull. Math. Biol. **65**, 641 (2003).
[13] K. Wiesenfeld, D. Pierson, E. Pantazelou, C. Dames, and F. Moss, Phys. Rev. Lett. **72**, 2125 (1994).
[14] V. V. Osipov and E. V. Ponizovskaya, Phys. Lett. A **369**, 238 (1998).
[15] A. Longtin and D. Chialvo, Phys. Rev. Lett. **81**, 4012 (1998).
[16] S. Massanés and C. J. Pérez Vicente, Phys. Rev. E **59**, 4490 (1999).
[17] B. Lindner and L. Schimansky-Geier, Phys. Rev. E **61**, 6103 (2000).
[18] V. V. Osipov and E. V. Ponizovskaya, Phys. Lett. A **271**, 191 (2000).
[19] C. Zhou, J. Kurths, and B. Hu, Phys. Rev. Lett. **87**, 098101 (2001).
[20] C. Zhou, J. Kurths, and B. Hu, Phys. Rev. E **67**, 030101 (2003).
[21] M. Perc and M. Marhl, Physica A **332**, 123 (2004).
[22] E. M. Izhikevich, Int. J. Bifurcation Chaos Appl. Sci. Eng. **10**, 1171 (2000).
[23] J. Rinzel and G. B. Ermentraut, in *Analysis of Neural Excitability and Oscillations. Methods in Neuronal Modeling, 1989*, edited by C. Koch and I. Segev (The MIT Press, Cambridge, 1989).
[24] E. M. Izhikevich, Neural Networks **14**, 883 (2001).
[25] L. Gammaitoni, M. Löcher, A. Bulsara, P. Hänggi, J. Neff, K. Wiesenfeld, W. Ditto, and M. E. Inchiosa, Phys. Rev. Lett. **82**, 4574 (1999).
[26] P. Parmananda, C. H. Mena, and G. Baier, Phys. Rev. E **66**, 047202 (2002).
[27] E. I. Volkov, E. Ullner, A. A. Zaikin, and J. Kurths, Phys. Rev. E **68**, 026214 (2003).
[28] E. Ulnner, A. Zaikin, R. Bascones, J. García-Ojalvo, and J. Kurths, Phys. Lett. A **312**, 348 (2003).
[29] P. Parmananda, H. Mahara, T. Amemiya, and T. Yamaguchi, Phys. Rev. Lett. **87**, 238302 (2001).
[30] M. Perc and M. Marhl, Chem. Phys. Lett. **376**, 432 (2003).
[31] S. Baer and T. Erneux, SIAM (Soc. Ind. Appl. Math.) J. Appl. Math. **46**, 721 (1986).
[32] F. Dumortier and R. Roussarie, Mem. Am. Math. Soc. **577**, 1 (1996).
[33] S. Schuster and M. Marhl, J. Biol. Syst. **9**, 291 (2001).
[34] W. H. Press, S. A. Teukolsky, W. T. Vetterling, and B. P. Flannery, *Numerical Recipes in C* (Cambridge University Press, Cambridge, 1995).
[35] J. Rinzel, in *Ordinary and Partial Differential Equations*, edited by B. D. Sleeman and R. J. Jarvis, Lecture Notes in Mathematics Berlin, 1985 (Springer, Berlin, 1985).
[36] R. Bertram, M. J. Butte, T. Kiemel, and A. Sherman, Bull. Math. Biol. **57**, 413 (1995).
[37] M. Perc and M. Marhl, Chaos, Solitons Fractals **18**, 759 (2003).
[38] J. Lisman, Trends Neurosci. **20**, 38 (1997).
[39] E. M. Izhikevich, BioSystems **67**, 95 (2002).
[40] E. M. Izhikevich, N. S. Desai, E. C. Walcott, and F. C. Hoppensteadt, Trends Neurosci. **26**, 161 (2003).
[41] E. Doedel, A. Champneys, T. Fairgrieve, and Y. Kuznetsov, *AUTO97: Continuation and Bifurcation Software for Ordinary Differential Equations* (Concordia University, Montreal, 1997).
[42] L. Holden and T. Erneux, SIAM (Soc. Ind. Appl. Math.) J. Appl. Math. **53**, 1045 (1993).
[43] L. Holden and T. Erneux, J. Math. Biol. **31**, 351 (1993).
[44] B. Hutcheon and Y. Yarom, Trends Neurosci. **23**, 216 (2000).
[45] P. Jung and P. Hänggi, Phys. Rev. A **44**, 8032 (1991).
[46] E. M. Izhikevich, SIAM Rev. **43**, 315 (2001).